
Using Deep Autoregressive Models as Causal Inference Engines

Daniel Jiwoong Im
Center for Data Science
New York University
ji641@nyu.edu

Kevin Zhang, Nakul Verma
Computer Science
Columbia University

Kyunghyun Cho
Center fo Data Science
New York University

Abstract

Existing causal inference (CI) models are limited to primarily handling low-dimensional confounders and singleton actions. We propose an autoregressive (AR) CI framework capable of handling complex confounders and sequential actions common in modern applications. We accomplish this by *sequencification*, transforming data from an underlying causal diagram into a sequence of tokens. This approach not only enables training with data generated from any DAG but also extends existing CI capabilities to accommodate estimating several statistical quantities using a *single* model. We can directly predict interventional probabilities, simplifying inference and enhancing outcome prediction accuracy. We demonstrate that an AR model adapted for CI is efficient and effective in various complex applications such as navigating mazes, playing chess endgames, and evaluating the impact of certain keywords on paper acceptance rates.

1 Introduction

Modelling causal relationships is important across various fields for informed decision-making [Holland, 1986, Cochran and Rubin, 1973, Pearl, 2010]. Existing causal inference (CI) algorithms are typically limited by their inability to handle high-dimensional covariates, actions, and outcomes [Louizos et al., 2017, Kumor et al., 2021, Im et al., 2021, Lu et al., 2022, Zhong et al., 2022]. Our goal in this work is to address this shortcoming and design a CI engine that is applicable to modern complex data involving high-dimensional variables.

We propose to leverage autoregressive (AR) models for estimating causal effects. As evidenced by large language models (LLMs), AR models can model complex relationships and scale well to vast quantities of data. Based on recent observations [Gupta et al., 2023, Zhang et al., 2024, Xu et al., 2024], fine-tuning pre-trained LLMs exploits existing knowledge from an internet-level text corpus.

We demonstrate that autoregressive language models are an effective and efficient statistical engine by treating observations as part of a data-generating process. To do this, we propose a method called *sequencification* for representing data with a known underlying causal diagram. A single model trained on sequencified data is able to use learned statistical estimates to answer a variety of causal questions. At inference, we can efficiently sample high-dimensional confounders and actions, enabling Monte Carlo estimation for approximating causal effects.

We conduct empirical studies on causal effect estimation for navigating mazes, playing chess endgames, and evaluating the impact of certain keywords on paper acceptance rates. Our experiments demonstrate that autoregressive language models are capable of (1) inferring causal effects

involving high-dimensional variables, (2) generalizing to unseen confounders and actions, and (3) utilizing pre-trained LLMs to accurately answer text-based causal questions. These results support the potential of autoregressive models for solving a broader array of CI problems.

2 Background

CI Problem Formulation. We are interested in studying interactions between the following set of variables: an observable confounder X , action A , and outcome Y . The causal relationship among these variables is represented as a directed acyclic graph where edges indicate direct effect among the variables (cf. Figure 1a). We compute the potential outcome when intervening on the action:

$$Y[A = a] = \mathbb{E}[Y \mid \text{do}(A = a)] = \sum_y y \sum_x p(Y = y \mid A = a, X = x)p(X = x),$$

where the do notation indicates an intervention on A . Typically, X and A are assumed to be low-dimensional. However, we are interested in modeling causal effects for high-dimensional variables and combinatorially large action spaces.¹

Language models. A large language model (LLM) is designed to predict and generate text based on linguistic patterns observed in a training corpus. LLMs estimate the probability of a sequence of tokens $\mathbf{v} = (w_1, \dots, w_T) \in \mathbb{V} \times \dots \times \mathbb{V}$ in an autoregressive manner, where \mathbb{V} is the vocabulary including special $\langle \text{start} \rangle$ and $\langle \text{end} \rangle$ tokens. The probability of the sequence \mathbf{v} is decomposed into the product of the next-token probabilities:

$$p(\mathbf{v}) = p(\langle \text{start} \rangle) \cdot \prod_{t=1}^T p(w_t \mid \mathbf{v}_{1:t-1}) \cdot p(\langle \text{end} \rangle \mid \mathbf{v}).$$

3 Language models as statistical inference engines

CI requires accurate estimation of several statistical quantities, as they are used to derive causal quantities. In this section, we describe how an autoregressive model can be turned into a statistical inference engine for any directed acyclic graph (DAG).

Causal graphs. We assume the underlying causal DAG $G = (\mathcal{V}, \mathcal{E})$ is known, where the vertices $V_i \in \mathcal{V}$ are random variables and the edges $E_{i \rightarrow j} \in \mathcal{E}$ represent conditional dependencies. The joint probability distribution is $p_G(V_1, V_2, \dots, V_M) = \prod_{i=1}^M p(V_i \mid \text{Pa}(V_i))$ where $\text{Pa}(V_i) = \{V_j \in \mathcal{V} \mid E_{j \rightarrow i} \in \mathcal{E}\}$ is the set of parent nodes of V_i . All variables in G are observed.

Sequencification. Suppose V_i takes value \mathbf{v}_i from its corresponding distribution. Define an injective function $\text{string}(\cdot)$ that represents \mathbf{v}_i as a string (or a sequence of tokens) of length L_i ,

$$\text{string}(\mathbf{v}_i) = (\langle \text{start}_i \rangle, w_1, w_2, \dots, w_{L_i-1}).$$

$\langle \text{start}_i \rangle$ is a special token indicating the beginning of the string representation for \mathbf{v}_i and is unique for each i . By looking at the start token, we can know which random variable $\text{string}(\mathbf{v}_i)$ represents

Let $\mathbf{t} = (V_{i_1}, V_{i_2}, \dots, V_{i_M})$ be a permutation of the random variables. We say \mathbf{t} is a *topological ordering* if V_i appears before V_j for all edges $E_{i \rightarrow j}$. Let \mathcal{T} be the set of all topological orderings.²

Suppose we have N samples drawn from the underlying causal DAG: $(\mathbf{v}_1^{(n)}, \mathbf{v}_2^{(n)}, \dots, \mathbf{v}_M^{(n)}) \sim p_G(V_1, V_2, \dots, V_M)$ for $n = 1, \dots, N$. We construct a string representation $\mathbf{s}^{(n)}$ for each sample by concatenating all random variable strings according to a topological ordering selected uniformly at random from \mathcal{T} .³ Formally, $\mathbf{t}^{(1)}, \mathbf{t}^{(2)}, \dots, \mathbf{t}^{(N)} \stackrel{i.i.d.}{\sim} \text{Uniform}(\mathcal{T})$ and

$$\mathbf{s}^{(n)} = \text{string}(\mathbf{v}_{i_1}^{(n)}) \oplus \text{string}(\mathbf{v}_{i_2}^{(n)}) \oplus \dots \oplus \text{string}(\mathbf{v}_{i_M}^{(n)}) \oplus \langle \text{end} \rangle,$$

¹Combinatorially large action space refers to the number of possible action sequences.

² \mathcal{T} is non-empty because a topological ordering always exists for a DAG.

³The ordering is selected randomly since the data may be generated from any topological ordering.

where $\mathbf{t}^{(n)} = (V_{i_1}, V_{i_2}, \dots, V_{i_M})$ and \oplus denotes string concatenation. Different samples may have different topological orderings. Since data is generated by ancestor sampling $\mathbf{v}_i^{(n)} \mid \text{Pa}(\mathbf{v}_i^{(n)})$, all random variables which causally affect string($\mathbf{v}_i^{(n)}$) appear before it in $\mathbf{s}^{(n)}$. We refer to the process of turning observed samples into a sequence of tokens as *sequencification*.

Autoregressive statistical inference engines. We train an AR language model parameterized by θ on the sequencified dataset $D = \{\mathbf{s}^{(n)}\}_{1 \leq n \leq N}$ by the minimizing negative log-likelihood:

$$J(\theta) = -\frac{1}{N} \sum_{n=1}^N \log p_{\theta}(\mathbf{s}^{(n)}) = -\frac{1}{N} \sum_{n=1}^N \sum_{t=1}^{|\mathbf{s}^{(n)}|} \log p_{\theta}(\mathbf{s}_t^{(n)} \mid \mathbf{s}_{1:t-1}^{(n)}) \quad (1)$$

where $|\cdot|$ denotes the length of a string and $\mathbf{s}_t^{(n)}$ is the t -th token in the string $\mathbf{s}^{(n)}$. The trained model can evaluate any conditional probability on G by computing $p_G(V_i \mid \text{Pa}(V_i)) \simeq p_{\theta}(\mathbf{v}_i \mid \text{Pa}(\mathbf{v}_i))$. This is efficiently computable by autoregressively sweeping through the sequence and calculating next-token probabilities using Monte Carlo estimation over the topological orders.

4 Language models as causal inference engines

In this section, we demonstrate how to infer causal effects using statistical quantities from a trained autoregressive model, effectively turning the model into a CI engine.

Causal quantity estimation. We express the CI problem as a corresponding language modelling task. Since our DAG consists of three variables, the observed confounder X , action A , and outcome Y , we sequencify the data as

$$\mathbf{s}^{(n)} = \text{string}(\mathbf{x}^{(n)}) \oplus \text{string}(\mathbf{a}^{(n)}) \oplus \text{string}(y^{(n)}) \oplus \langle \text{end} \rangle,$$

where $\mathbf{x}^{(n)}$, $\mathbf{a}^{(n)}$, and $y^{(n)}$ belong to the n^{th} data sample. In our formulation, $\mathbf{x}^{(n)}$ and $\mathbf{a}^{(n)}$ may be high-dimensional and combinatorially large. Without loss of generality, the outcome variable Y is a scalar and treated as a single token.

We train an AR model to compute the distribution of Y after intervening on A . This is typically intractable when X is high-dimensional or when the action space is large. However, we can address this by sampling from the model $p_{\theta}(X)$ and using Monte Carlo estimation.

$$p_{\theta}(Y = y \mid \text{do}(A = \mathbf{a})) = \sum_{\mathbf{x}} p_{\theta}(y \mid A = \mathbf{a}, \mathbf{x}) p_{\theta}(\mathbf{x}) \simeq \frac{1}{S} \sum_{s=1}^S p_{\theta}(y \mid A = \mathbf{a}, \mathbf{x}^{(s)}). \quad (2)$$

where $\mathbf{x}^{(s)} \sim p(X)$. Furthermore, we can intervene on a subsequence \mathbf{a}_1 (i.e. a prefix of \mathbf{a}) even when the action space is combinatorially large. Let $A = A_1 \oplus A_2$, then by marginalizing out A_2 ,

$$p(Y = y \mid \text{do}(A_1 = \mathbf{a}_1)) = \sum_{\mathbf{x}} \sum_{\mathbf{a}_2} p_{\theta}(y \mid A_1 = \mathbf{a}_1, A_2 = \mathbf{a}_2, \mathbf{x}) p_{\theta}(\mathbf{a}_2 \mid \mathbf{a}_1, \mathbf{x}) p_{\theta}(\mathbf{x}) \quad (3)$$

$$\simeq \frac{1}{S} \sum_{s=1}^S p_{\theta}(y \mid \mathbf{a}_1, \mathbf{a}_2^{(s)}, \mathbf{x}^{(s)}) \quad (4)$$

where $\mathbf{x}^{(s)} \sim p(X)$ and $\mathbf{a}_2^{(s)} \sim p(A_2 \mid \mathbf{a}_1, \mathbf{x}^{(s)})$. Similarly, we can condition on partial confounders \mathbf{x}_1 , (i.e. prefix of \mathbf{x}). Let $X = X_1 \oplus X_2$, then by marginalizing out X_2 ,

$$p(Y = y \mid \text{do}(A = \mathbf{a}), \mathbf{x}_1) = \sum_{\mathbf{x}_2} p_{\theta}(y \mid A = \mathbf{a}, \mathbf{x}_2, \mathbf{x}_1) p_{\theta}(\mathbf{x}_2 \mid \mathbf{x}_1) \quad (5)$$

$$\simeq \frac{1}{S} \sum_{s=1}^S p_{\theta}(y \mid A = \mathbf{a}, \mathbf{x}_2^{(s)}, \mathbf{x}_1) \quad (6)$$

where $\mathbf{x}_2^{(s)} \sim p(X_2 \mid X_1 = \mathbf{x}_1)$. The causal diagrams for these scenarios are depicted in Figure 1.

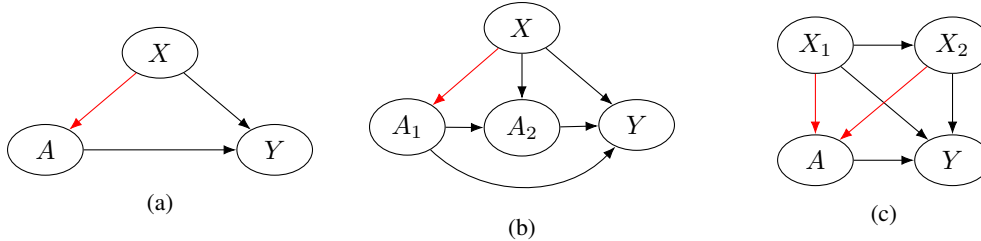


Figure 1: Causal diagrams for intervening on the action (a), partial action (b), and conditioning on a prefix of the confounders (c). Arrows in red are ones that are blocked when intervening on the corresponding action.

All causal quantities are computed by a *single* language model trained on sequencified observations. We can efficiently sample and compute conditional $p(Y | A = \mathbf{a})$, interventional $p(Y | \text{do}(A = \mathbf{a}))$, partial interventional $p(Y | \text{do}(A = \mathbf{a}_1))$, and conditional interventional $p(Y | \text{do}(A = \mathbf{a}), X_1 = \mathbf{x}_1)$ distributions with a unified model.

One limitation of our approach lies in conditioning or intervening on the non-prefix of a variable. Despite the difficulty of non-prefix intervention, existing literature offers potential strategies to address this issue [Donahue et al., 2020, Welleck et al., 2019, Berenberg et al., 2022]. However, we defer this problem for future work.

5 Related work

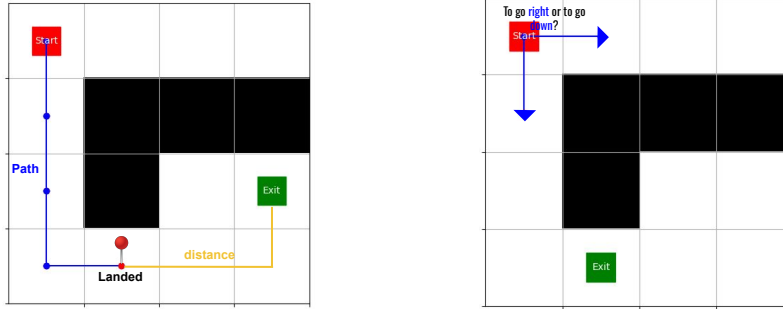
Previous works have explored using autoregressive models for inferring causal effects. Here, we give a brief overview of the studies.

Sequencification for statistical engines. Various machine learning disciplines have employed linearized observations for their tasks. In natural language processing (NLP), linearization (which we call sequencification) has been used to encode a syntactic tree into a sequence for building a language model-based parser [Vinyals et al., 2015, Liu et al., 2022, Sheng et al., 2023]. In reinforcement learning (RL), an episode can be encoded into a sequence of states, actions, and reward variables. An autoregressive model is then trained on these sequences to capture relationships among the variables [Chen et al., 2021, Janner et al., 2021]. These instances suggest that AR models trained on sequencified data adeptly learn statistical dependencies among multiple variables.

Language models as causal engines. One challenging aspect of CI in high-dimensional space is satisfying positivity constraints [D’Amour et al., 2021, Tu and Li, 2022, Egami et al., 2022, Gui and Veitch, 2022]. Despite this limitation, previous studies use techniques from NLP, such as topic models [Sridhar and Getoor, 2019, Mozer et al., 2020], latent variable models [Keith et al., 2020], and contextual embeddings [Veitch et al., 2019, 2020], to produce low-dimensional embeddings that may satisfy positivity.

Besides applying NLP techniques to reduce the dimensionality of observations, we can use natural language as a proxy for observed confounders. For instance, Roberts et al. [2020] applies a text-matching algorithm using contextual embeddings and topic models to estimate causal effects given a proxy text. Furthermore, with sufficiently large models and text corpuses, LLMs can generalize to unseen knowledge [Chowdhery et al., 2023]. Hence, we rely on pre-trained LLMs to take advantage of the prior model knowledge and train better statistical inference engines. However, further studies need to be conducted to understand the performance of LLMs for estimating causal quantities.

Deep learning for causal engines. Different types of deep neural networks have been proposed for causal inference. Often representation learning for CI consists of a regularization term that encourages better generalization for counterfactual actions [Shalit et al., 2017, Johansson et al., 2018, Wang and Jordan, 2021]. Deep latent variable CI models learn stochastic latent variables to model potential outcomes with a richer distribution [Louizos et al., 2017, Kocaoglu et al., 2017, Im et al., 2021]. In the case of deep autoregressive models, Monti et al. [2020] introduces an AR flow



(a) What's the potential outcome given a path? (b) Is it better to go "Right" or "Down"?

Figure 2: Illustrations of the two different types of maze problems: we answer interventional questions given a path (a) and given a partial path (b).

model that learns an invertible density transformation from one variable to another. This enables direct computation of interventional and counterfactual distributions without the need for complex latent variable manipulations. Garrido et al. [2021] uses neural AR density estimators [Larochelle and Murray, 2011] to model causal mechanisms and predict causal effects using Pearl’s do-calculus.

Existing limitations. Previous works exhibit two weaknesses compared to our proposed approach. First, most of the methods have been validated using only low-dimensional setups. Second, these studies often only work with a predefined number of variables. In contrast, our approach for using an autoregressive model works on high dimensional and combinatorially large variables and is applicable to causal diagrams with of any number of variables.

6 Experiments

We demonstrate the effectiveness of our proposed approach for estimating causal effects with both randomized and non-randomized data. Our experiments are designed to showcase the capability to (1) infer potential outcomes with sequential actions and high-dimensional confounders, (2) efficiently approximate potential outcomes, and (3) utilize existing knowledge from a pre-trained LLM. We conduct our analysis using three environments: a maze environment examining navigational decisions, a chess environment focusing on strategic moves in king versus king-rook endgames, and the PeerRead dataset that investigates the influence of theorem existences on academic paper acceptances. These diverse settings allow us to test the effectiveness and robustness of our approaches for CI. We train a vanilla transformer [Vaswani et al., 2017] for all AR models unless otherwise specified. Further details regarding model architecture and training are provided in Appendix A.

6.1 Maze experiments

We create a synthetic maze dataset to investigate the causal effect of traversing paths within a maze. The objective is to determine the distance to the exit after following a path. The confounding variable X is the start and end positions, the action A is the sequence of moves in a path, and the outcome y is the distance from the final position to the exit.⁴ We compute potential outcomes in two settings: given a path (cf. Figure 2a) and given a partial path (cf. Figure 2b). The positions of the obstacles are unknown to the model. We run a randomized controlled trial (RCT) in order to determine the ground truth potential outcomes in all experiments.

We train three autoregressive models on three separate datasets and evaluate them in the previously described two settings. The first dataset is the RCT dataset, where we randomly select an exit point and sequence of actions. The remaining two non-RCT datasets are produced using two distinct policy functions respectively. The first, termed *offline*, only includes paths predicted by a neural network trained to identify optimal maze routes. The second dataset is created as a mixture of the

⁴ y is the shortest distance in the maze while avoiding obstacles, not necessarily the Hamming distance.

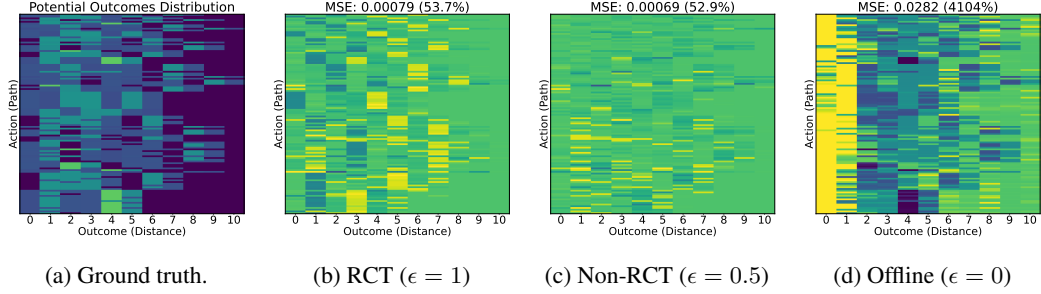


Figure 3: (a) depicts ground truth potential outcome for all valid paths (y -axis) and outcomes (x -axis). (b-d) shows the MSE between the ground truth and model estimates for various ϵ values and its relative error with respect to the ground truth. The estimates closely align with the ground truth for all datasets except for the AR trained with a non-RCT dataset ($\epsilon = 0$).

RCT and the offline dataset at different a mixing rate ϵ . In total, we construct three datasets with $\epsilon \in \{0, 0.5, 1\}$, where $\epsilon = 1$ and $\epsilon = 0$ correspond to the RCT and offline dataset respectively.

6.1.1 Causal inference using sequential actions

We estimate potential outcomes for possible paths in a 4×4 maze with a fixed starting point and a maximum length of 6. The maze dimensions are kept small to calculate exact potential outcomes. Figure 3 (a) shows the ground truth potential outcomes for all valid paths. We also compute the mean square error (MSE) and relative error to the empirical RCT estimate. In Figure 3 (b-c), we observe that the estimates closely align with the ground truth for all datasets except $\epsilon = 0$. This is because the offline model trained only from optimal moves fails to predict outcomes given a non-optimal path. Hence, autoregressive models generalize even with non-RCT data unless the observed actions are nearly deterministic. Additional experiments on a 6×6 maze are included in Appendix B.

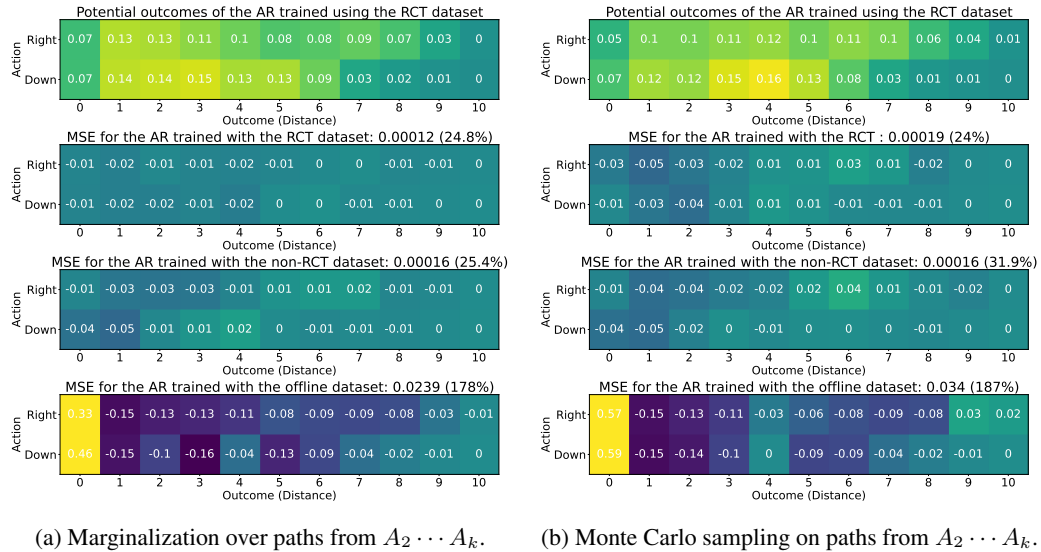


Figure 4: Potential outcome MSE between ground truth and model estimates for moving ‘right’ vs. ‘down’ first. Both the *exact model estimate* (a) and *approximate model estimate* (b) are shown. From comparing (a) and (b), the Monte Carlo approximation has similar potential outcome results.

6.1.2 Causal inference using subsequential actions

We consider another question: for a fixed starting state, is it better to go down or right in general (cf. Figure 2b)? To answer this, we compute the potential outcome of moving down or right initially.

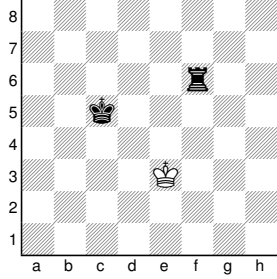


Figure 5: An example chess endgame position. The probability of moving the king for Black is 0.5, 0.25, and 0.8 for the RCT, non-RCT₁, and non-RCT₂ policies respectively.

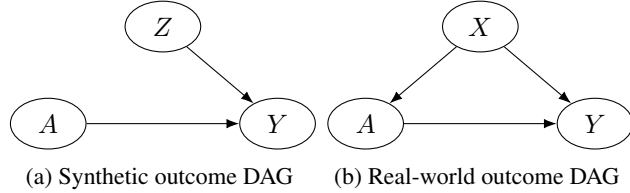


Figure 6: Causal diagrams for the PeerRead dataset, where X denotes the paper abstract, Z is title buzziness, A indicates the presence of a theorem, and Y is the acceptance outcome. We generate synthetic outcomes using Z and A in (a); however, the true causal factors are X and A depicted in (b).

This task is prohibitive for most non-autoregressive CI models as they treat the path as a singular variable. Our model is capable of intervening on *any subsequence of actions* because the conditional probability of a single action given its parents is computable.

To compute the potential outcome, we marginalize over subsequent actions as shown in Equation 3. Since the paths may be intractable without limiting the maximum length, we cap the longest path to 16 moves as there are a total of 16 positions in the maze. To compare the exact estimates with the Monte Carlo approximations, we report both quantities derived from Equation 3 and 4, and denote them as *exact model estimate* and *approximate model estimate* respectively.

Figure 4 shows the potential outcome estimate of moving right or down initially. The distribution is more concentrated towards smaller distances for moving down and more uniform for moving right. Thus, going down is a better choice for the first move. Furthermore, we observe that $\epsilon = 0$ and 0.5 perform similarly, while $\epsilon = 1$ has a larger MSE because of strictly non-RCT data. More importantly, comparing the exact and approximate model estimates, the Monte Carlo approximation yields similar potential outcomes.

6.2 Chess endgame experiments

In this experiment, we analyze a synthetic chess dataset featuring king vs. king-rook endgames with White to move and Black holding the rook. We consider the question: which pieces should Black move on the first two turns to checkmate White the quickest? Using an autoregressive model, we accurately estimate potential outcomes and identify the best action sequence for Black. Furthermore, we use Monte Carlo sampling to obtain better estimates when provided a subset of the data. By answering a query whose solution is not readily apparent, we demonstrate the capability of our proposed causal engine in a more complex and realistic scenario compared to the maze.

Each endgame comprises a two-move chess game, potentially incomplete. The covariate X is the initial piece position. The action $A = a_1, a_2, a_3, a_4$ represents alternating White and Black moves. Since we consider Black’s perspective, we are interested in causal quantities involving a_2 and a_4 . We assume Black plays optimally after selecting which piece to maneuver, so each action only dictates whether to move the king or the rook, not to which location. The outcome variable y is the number of additional moves required to checkmate with optimal play.⁵ We evaluate the ground-truth outcome using the chess engine Stockfish. An example endgame is shown in Figure 5.

We construct three training datasets: one RCT and two non-RCT sets, denoted non-RCT₁ and non-RCT₂, with distinct action policies. The RCT dataset uniformly at random selects between moving the king or rook. non-RCT₁ and non-RCT₂ policy functions are respectively defined as

$$\pi_1(a_2, a_4 = \text{king}) = \frac{d}{16}, \quad \pi_2(a_2, a_4 = \text{king}) = \begin{cases} 0.8 & \text{if black king is in center } 4 \times 4 \text{ square} \\ 0.2 & \text{otherwise} \end{cases}$$

⁵In the event of a draw, the outcome is set to 50 due to the 50-move rule.

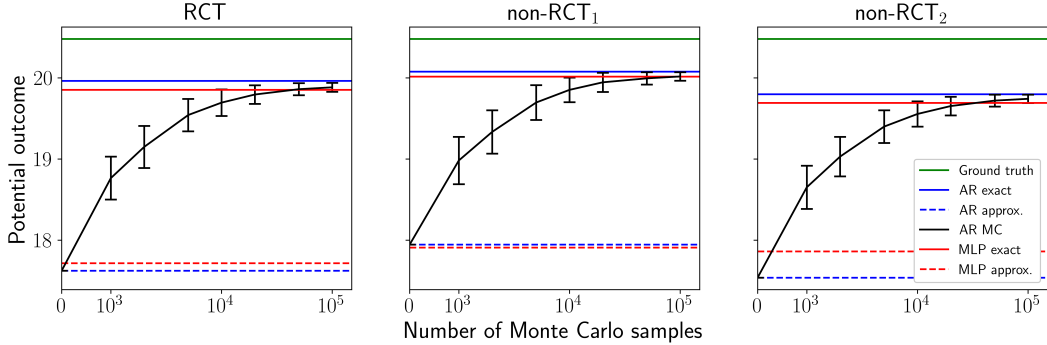


Figure 7: Potential outcome estimates for rook-king. The *exact model estimate* uses all 223,660 valid starting positions as test samples, whereas the *approximate* and *Monte Carlo estimates* use 1,000 randomly selected samples. Each Monte Carlo estimate was repeated 1,000 times and error bars indicate one standard deviation. By additionally sampling from $p_\theta(X)$, the AR Monte Carlo estimate approaches the AR exact estimate. Conversely, MLP cannot perform sampling on $p_\theta(X)$.

where d is the Hamming distance between the kings. π_1 encourages the two kings to be closer while π_2 pushes the Black king towards the edge of the board, both of which is required for checkmate. We employ two distinct policies for White between training and testing to evaluate out-of-distribution generalization. White plays uniformly at random over non-optimal moves (unless there are no such legal moves) for the training dataset and only plays optimally in the test set.

We calculate the ground-truth potential outcomes for all actions and compare them with three different model estimates: the *exact model estimate* using the entire test dataset, *approximate model estimate* using a subset of the test data, and *Monte Carlo model estimate* using the same data subset, but additionally generating samples from the model. The approximate and Monte Carlo estimates correspond to a real-world setting, since obtaining many RCT samples is difficult. Figure 7 shows that as we increase the number of samples for Monte Carlo approximation, the potential outcome estimates approach to exact estimate. One reason for the gap between ground truth and AR exact model estimate is due to a distribution shift in $p(A | X)$ between the training and test data. The potential outcomes for the remaining actions are provided in Appendix C. By comparing all potential outcome estimates, we correctly answer our proposed counterfactual query and conclude that moving the rook twice initially is best for Black.

6.3 PeerRead experiments

In this experiment, we use the PeerRead dataset [Kang et al., 2018] to estimate causal effects in a semi-realistic context with high-dimensional confounders. The dataset consists of paper draft submissions to leading computer science conferences such as NeurIPS, ICML, and ICLR, along with acceptance/rejection decisions. We examine the impact of including "theorems" on the likelihood of acceptance. Building on prior work, we focus on computational linguistics, machine learning, and artificial intelligence papers submitted between 2007 and 2017 [Veitch et al., 2020].

The covariate X is the paper’s abstract text, the action A is a binary variable specifying the presence of the keyword “theorem”, and the outcome Y is a binary variable indicating acceptance or rejection. To address inaccessible real-world counterfactual outcomes, we follow prior methods by generating synthetic outcomes using the action A and the title buzziness Z (whether the title contains “deep”, “neural”, or “adversarial net”), as shown in Figure 6. For instance, $z = 1$ and $a = 1$ likely denote a deep learning paper featuring a theorem, whereas $z = 0$ and $a = 1$ might be a theoretical machine learning paper (or a deep learning paper with a theorem but lacking a buzzy title). [Veitch et al., 2020] has established a correlation between title buzziness and the text.

We compare our proposed approach against Causal-Bert (C-BERT) from [Veitch et al., 2020].⁶ Just like C-BERT, we fine-tune the pre-trained BERT model on our sequencified representations for a

⁶C-BERT learns causally sufficient embeddings, low-dimensional document representations that preserve sufficient information for causal identification and allow for efficient estimation of causal effects.

Table 1: PeerRead ATT performance for low, medium, and high confounding. The relative error is indicated in parenthesis. Our Deep Autoregressive Causal Inference Engine BERT (DARCIE-BERT) model has the lowest relative error, followed by DARCIE-GPT. Both demonstrate a significant improvement over methods. However, training DARCIE-GPT from scratch fails to identify causal effects due to lacking understanding of the text.

	Confounding level		
	Low	Medium	High
Ground truth	0.062	0.059	0.028
Computed biased	0.065 (4.8%)	0.097 (68%)	0.160 (470%)
Reported biased [Veitch et al., 2020]	0.08 (30%)	0.15 (150%)	0.16 (471%)
MLP $\hat{\psi}^Q$	0.05 (20%)	0.1 (70%)	0.3 (970%)
C-BERT $\hat{\psi}^{\text{plugin}}$	0.10 (61%)	0.09 (53%)	0.05 (78%)
C-BERT $\hat{\psi}^Q$	0.09 (45%)	0.07 (19%)	0.04 (42%)
DARCIE-GPT2 (No pre-train)	0.001 (98%)	0.002 (97%)	0.001 (96%)
DARCIE-BERT (Ours)	0.052 (16%)	0.050 (15%)	0.023 (18%)
DARCIE-GPT2 (Ours)	0.050 (20%)	0.044 (25%)	0.020 (29%)

fair comparison. We randomly sample subsections of the abstract and fine-tune BERT as if it is a next-token prediction model. Additionally, we use GPT-2 (referred to as GPT) as another pre-trained model [Radford et al., 2019] which has a comparable parameter size to BERT.

Following the original experiment design, we report the Average Treatment Effect on the Treated (ATT) across three confounding levels: low, medium, and high. A positive ATT indicates that including a theorem increases the paper’s chance of acceptance. Table 1 demonstrates that our approach outperforms C-BERT and other benchmarks by significant margins.⁷ The major difference between C-BERT and our approach is that we do not distinguish between learning representations and the outcome prediction network, and instead train one model to do both. In contrast, C-BERT uses multiple objective functions and additional architectural layers.

Our proposed framework is able to exploit the existing knowledge in pre-trained LLMs. Training GPT from scratch fails to identify causal effects, whereas fine-tuning GPT does. By leveraging existing language models, we can estimate causal quantities even under the high-dimensional confounding setting. Consequently, our approach applies to a wider variety of CI tasks and is more capable than non-autoregressive causal models.

7 Conclusion

In this work, we propose an autoregressive model framework for causal inference capable of handling high-dimensional and combinatorially large variables. In our approach, the key idea is to sequencify data according to the underlying causal DAG and train an autoregressive model to learn conditional distributions. Our experiments show that this method is a unified and robust approach to inferring causal effects.

Despite its effectiveness, our approach has three primary limitations. Firstly, the underlying causal graph must be known. Secondly, all variables in the graph must be observed. Lastly, our approach only supports conditioning or intervening on the prefix of a variable. We leave investigations on overcoming these limitations for future work.

Broader Impact Statement

Our research introduces an deep autoregressive model framework for causal inference, designed to handle high-dimensional data. This method potentially enables scientific discoveries and promotes social fairness by uncovering causal relationships among key variables. However, causal modeling relies on strong assumptions and may not always identify the true causal structure of observational data. Nonetheless, we believe our framework promotes a positive societal impact due to its effectiveness and flexibility over a wider variety of CI applications.

⁷We explain the strong performance despite different synthetic and real-world causal graphs in Appendix D.

References

- D. Berenberg, J. H. Lee, S. Kelow, J. W. Park, A. Watkins, V. Gligorijević, R. Bonneau, S. Ra, and K. Cho. Multi-segment preserving sampling for deep manifold sampler, 2022.
- L. Chen, K. Lu, A. Rajeswaran, K. Lee, A. Grover, M. Laskin, P. Abbeel, A. Srinivas, and I. Mor-datch. Decision transformer: Reinforcement learning via sequence modeling, 2021.
- A. Chowdhery, S. Narang, J. Devlin, M. Bosma, G. Mishra, and A. R. et al. Palm: Scaling language modeling with pathways. *Journal of Machine Learning Research*, 24(240):1–113, 2023. URL <http://jmlr.org/papers/v24/22-1144.html>.
- W. G. Cochran and D. B. Rubin. Controlling bias in observational studies: A review. *The Indian Journal of Statistics, Series A*, 35:417–446, 1973. doi: JSTOR,<http://www.jstor.org/stable/25049893>.
- C. Donahue, M. Lee, and P. Liang. Enabling language models to fill in the blanks, 2020.
- A. D’Amour, P. Ding, A. Feller, L. Lei, and J. Sekhon. Overlap in observational studies with high-dimensional covariates. *Journal of Econometrics*, 221(2):644–654, 2021.
- N. Egami, C. J. Fong, J. Grimmer, M. E. Roberts, and B. M. Stewart. How to make causal inferences using texts. *Science Advances*, 8(42):eabg2652, 2022.
- S. Garrido, S. Borysov, J. Rich, and F. Pereira. Estimating causal effects with the neural autoregressive density estimator. *Journal of Causal Inference*, 9(1):211–228, 2021. doi: doi: 10.1515/jci-2020-0007. URL <https://doi.org/10.1515/jci-2020-0007>.
- L. Gui and V. Veitch. Causal estimation for text data with (apparent) overlap violations. *arXiv preprint arXiv:2210.00079*, 2022.
- K. Gupta, B. Th’erien, A. Ibrahim, M. L. Richter, Q. G. Anthony, E. Belilovsky, I. Rish, and T. Lesort. Continual pre-training of large language models: How to (re)warm your model? *ArXiv*, abs/2308.04014, 2023. URL <https://api.semanticscholar.org/CorpusID:260704601>.
- P. W. Holland. Statistics and causal inference. *Journal of the American Statistical Association*, 81(396):945–960, 1986. doi: 10.1080/01621459.1986.10478354. URL <https://www.tandfonline.com/doi/abs/10.1080/01621459.1986.10478354>.
- D. j. I. Im, K. Cho, and N. Razavian. Causal effect variational autoencoder with uniform treatment for overcoming covariate shifts. In *arXiv preprint arXiv:2111.08656*, 2021.
- M. Janner, Q. Li, and S. Levine. Offline reinforcement learning as one big sequence modeling problem. In M. Ranzato, A. Beygelzimer, Y. Dauphin, P. Liang, and J. W. Vaughan, editors, *Advances in Neural Information Processing Systems*, volume 34, pages 1273–1286. Curran Associates, Inc., 2021. URL https://proceedings.neurips.cc/paper_files/paper/2021/file/099fe6b0b444c23836c4a5d07346082b-Paper.pdf.
- F. D. Johansson, N. Kallus, U. Shalit, and D. A. Sontag. Learning weighted representations for generalization across designs. *arXiv: Machine Learning*, 2018.
- D. Kang, W. Ammar, B. Dalvi, M. van Zuylen, S. Kohlmeier, E. Hovy, and R. Schwartz. A dataset of peer reviews (PeerRead): Collection, insights and NLP applications. In M. Walker, H. Ji, and A. Stent, editors, *Proceedings of the 2018 Conference of the North American Chapter of the Association for Computational Linguistics: Human Language Technologies, Volume 1 (Long Papers)*, pages 1647–1661, New Orleans, Louisiana, June 2018. Association for Computational Linguistics. doi: 10.18653/v1/N18-1149. URL <https://aclanthology.org/N18-1149>.
- K. A. Keith, D. Jensen, and B. O’Connor. Text and causal inference: A review of using text to remove confounding from causal estimates, 2020.
- M. Kocaoglu, K. Shanmugam, and E. Bareinboim. Experimental design for learning causal graphs with latent variables. In I. Guyon, U. V. Luxburg, S. Bengio, H. Wallach, R. Fergus, S. Vishwanathan, and R. Garnett, editors, *Advances in Neural Information Processing Systems*, volume 30. Curran Associates, Inc., 2017. URL <https://proceedings.neurips.cc/paper/2017/file/291d43c696d8c3704cdbe0a72ade5f6c-Paper.pdf>.

- D. Kumor, J. Zhang, and E. Bareinboim. Sequential causal imitation learning with unobserved confounders. In M. Ranzato, A. Beygelzimer, Y. Dauphin, P. Liang, and J. W. Vaughan, editors, *Advances in Neural Information Processing Systems*, volume 34, pages 14669–14680. Curran Associates, Inc., 2021. URL <https://proceedings.neurips.cc/paper/2021/file/7b670d553471ad0fd7491c75bad587ff-Paper.pdf>.
- H. Larochelle and I. Murray. The neural autoregressive distribution estimator. In G. Gordon, D. Dunson, and M. Dudík, editors, *Proceedings of the Fourteenth International Conference on Artificial Intelligence and Statistics*, volume 15 of *Proceedings of Machine Learning Research*, pages 29–37, Fort Lauderdale, FL, USA, 11–13 Apr 2011. PMLR. URL <https://proceedings.mlr.press/v15/larochelle11a.html>.
- T. Liu, Y. E. Jiang, N. Monath, R. Cotterell, and M. Sachan. Autoregressive structured prediction with language models. In Y. Goldberg, Z. Kozareva, and Y. Zhang, editors, *Findings of the Association for Computational Linguistics: EMNLP 2022*, pages 993–1005, Abu Dhabi, United Arab Emirates, Dec. 2022. Association for Computational Linguistics. doi: 10.18653/v1/2022.findings-emnlp.70. URL <https://aclanthology.org/2022.findings-emnlp.70>.
- C. Louizos, U. Shalit, J. Mooij, D. Sontag, R. Zemel, and M. Welling. Causal effect inference with deep latent-variable models. In *arXiv preprint arXiv:1705.08821*, 2017.
- Z. Lu, Y. Cheng, M. Zhong, G. Stoian, Y. Yuan, and G. Wang. *Causal Effect Estimation Using Variational Information Bottleneck*, pages 288–296. 12 2022. ISBN 978-3-031-20308-4. doi: 10.1007/978-3-031-20309-1-25.
- R. P. Monti, I. Khemakhem, and A. Hyvarinen. Autoregressive flow-based causal discovery and inference, 2020.
- R. Mozer, L. Miratrix, A. R. Kaufman, and L. J. Anastasopoulos. Matching with text data: An experimental evaluation of methods for matching documents and of measuring match quality. *Political Analysis*, 28(4):445–468, 2020.
- J. Pearl. An introduction to causal inference. *The international journal of biostatistics*, 6:1557–4679, 2010.
- A. Radford, J. Wu, R. Child, D. Luan, D. Amodei, and I. Sutskever. Language models are unsupervised multitask learners. 2019.
- M. E. Roberts, B. M. Stewart, and R. A. Nielsen. Adjusting for confounding with text matching. *American Journal of Political Science*, 64(4):887–903, 2020.
- U. Shalit, F. D. Johansson, and D. Sontag. Estimating individual treatment effect: Generalization bounds and algorithms. ICML’17, page 3076–3085. JMLR.org, 2017.
- K. Sheng, Z. Wang, Q. Zhao, X. Jiang, and G. Zhou. A unified framework for synaesthesia analysis. In H. Bouamor, J. Pino, and K. Bali, editors, *Findings of the Association for Computational Linguistics: EMNLP 2023*, pages 6038–6048, Singapore, Dec. 2023. Association for Computational Linguistics. doi: 10.18653/v1/2023.findings-emnlp.401. URL <https://aclanthology.org/2023.findings-emnlp.401>.
- D. Sridhar and L. Getoor. Estimating causal effects of tone in online debates. In *Proceedings of the Twenty-Eighth International Joint Conference on Artificial Intelligence*, 2019.
- H. Tu and Y. Li. An overview on controllable text generation via variational auto-encoders. *ArXiv*, abs/2211.07954, 2022. URL <https://api.semanticscholar.org/CorpusID:253523104>.
- A. Vaswani, N. Shazeer, N. Parmar, J. Uszkoreit, L. Jones, A. N. Gomez, Ł. Kaiser, and I. Polosukhin. Attention is all you need. *Advances in neural information processing systems*, 30, 2017.
- V. Veitch, D. Sridhar, and D. M. Blei. Using text embeddings for causal inference. *ArXiv*, abs/1905.12741, 2019. URL <https://api.semanticscholar.org/CorpusID:170079051>.

- V. Veitch, D. Sridhar, and D. Blei. Adapting text embeddings for causal inference. In J. Peters and D. Sontag, editors, *Proceedings of the 36th Conference on Uncertainty in Artificial Intelligence (UAI)*, volume 124 of *Proceedings of Machine Learning Research*, pages 919–928. PMLR, 03–06 Aug 2020. URL <https://proceedings.mlr.press/v124/veitch20a.html>.
- O. Vinyals, L. Kaiser, T. Koo, S. Petrov, I. Sutskever, and G. Hinton. Grammar as a foreign language. In *NIPS*, 2015. URL <http://arxiv.org/abs/1412.7449>.
- Y. Wang and M. I. Jordan. Desiderata for representation learning: A causal perspective, 2021.
- S. Welleck, K. Brantley, H. D. Iii, and K. Cho. Non-monotonic sequential text generation. In K. Chaudhuri and R. Salakhutdinov, editors, *Proceedings of the 36th International Conference on Machine Learning*, volume 97 of *Proceedings of Machine Learning Research*, pages 6716–6726. PMLR, 09–15 Jun 2019. URL <https://proceedings.mlr.press/v97/welleck19a.html>.
- M. Xu, W. Yin, D. Cai, R. Yi, D. Xu, Q. Wang, B. Wu, Y. Zhao, C. Yang, S. Wang, et al. A survey of resource-efficient llm and multimodal foundation models. *arXiv preprint arXiv:2401.08092*, 2024.
- P. Zhang, G. Zeng, T. Wang, and W. Lu. Tinyllama: An open-source small language model, 2024.
- K. Zhong, F. Xiao, Y. Ren, Y. Liang, W. Yao, X. Yang, and L. Cen. Descn: Deep entire space cross networks for individual treatment effect estimation. *Proceedings of the 28th ACM SIGKDD Conference on Knowledge Discovery and Data Mining*, 2022.

A Architecture and training

The maze experiments were conducted on a single NVIDIA GeForce RTX 1080 TI. All models for the chess and PeerRead experiments were trained on a single NVIDIA GeForce RTX 3090 in four and eight hours respectively.

Maze experiments. All three datasets contain 50,000 sequencified data points. We use a vanilla transformer model for the policy and outcome prediction networks consisting of 4 block layers, 32 dimensional 4 multi-heads, and a batch size of 100. We trained 20,000 epochs using Adam for the CI model and 2000 epochs for the policy neural network to avoid overfitting.

Chess endgame experiments. We use a 512-dimensional vanilla transformer, comprising 6 block layers and 8 attention heads. The training task is next-token prediction using the tokenized representation. We train for 200 epochs using the Adam optimizer with a batch size of 4096. The learning rate was selected to be as large as possible without overfitting.

For the training dataset, we sample 500k two-move chess games for each dataset based on Black’s policy function. The test dataset encompasses every game for all 223,660 legal starting positions and all four possible Black actions (king-king, king-rook, rook-king, rook-rook). We sequencify the data by assigning a unique token to every square, legal king and rook move, and outcome.

PeerRead experiments. We fine-tuned our models from the pre-trained BERT and GPT base model checkpoints.⁸ We employed a two-phase training process for BERT, analogous to the training of C-BERT. In the initial phase, we focused on training BERT to generate abstracts. The second phase involves training BERT to generate full sequences that include both actions and outcomes. The initial phase is not required for GPT since it was pre-trained on next-token prediction, so training GPT is streamlined into one step. This method ensures a gradual enhancement of the models’ generative abilities, tailored specifically to the PeerRead corpus.

For all training phases, we train for 100 epochs using the Adam optimizer with a batch size of 16. The learning rate and weight decay was chosen at large and small as possible respectively without overfitting. While training the GPT model from scratch, we notice that overfitting occurs regardless of the learning rate or weight decay.

We elaborate on the synthetic outcome generation process (cf. Figure 6). Following [Veitch et al., 2020], the synthetic outcome is expressed as

$$y_i = \text{Bernoulli}(\sigma(0.25 \cdot t_i + \beta(\pi(z_i) - 0.2)))$$

where σ is a sigmoid function, $\pi(Z)$ is a proportional to $p(A = 1 | Z)$ in each paper, and β controls the level of confounding. Low, medium, and high confounding levels in this work correspond to $\beta = 1, 5,$ and 25 respectively. Higher β indicates the outcome is more correlated to the title buzziness Z instead of the action A , so the ground-truth ATT is smaller. Note that the PeerRead dataset is imbalanced with more non-buzzy papers than buzzy ones.

B Maze extra experiments

B.1 Comparing two paths on 6x6 Maze

We consider a larger 6×6 maze featuring two distinct paths as illustrated in Figure 8. For this setup, we compute potential outcomes given a set of valid exit points instead of a single exit point. During the training phase, the exit location is randomly chosen within the maze; however, during testing, it is restricted to the bottom-right quadrant. Taking the red path is far away from all but one exit, whereas taking the blue path is close to all but one exit. The first heat map in Figure 9 depicts potential outcome estimates for both paths, with outcomes ranging from 0-2 and 16 for the blue path and 0-15 to 17 for the red path, aligning with the intuition from Figure 8. Subsequent heat maps display the potential outcome MSE.

⁸BERT-Base is available at https://huggingface.co/google/bert_uncased_L-12_H-768_A-12 and GPT is available at <https://huggingface.co/openai-community/gpt2>.

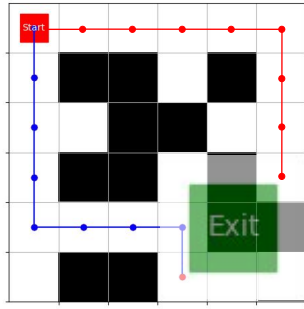


Figure 8: Is it better to take red vs. blue path given exit cells?

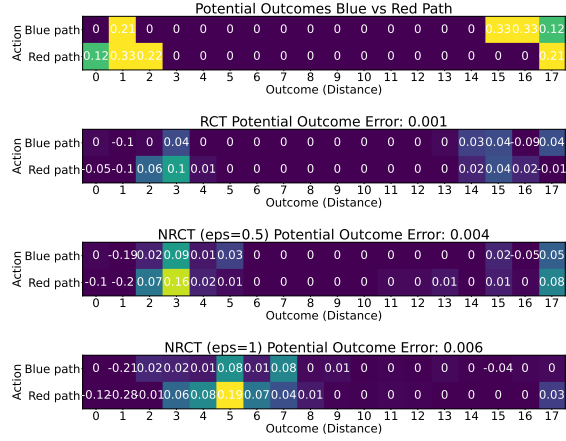


Figure 9: (Row 1) Potential outcomes for taking blue and red paths (ref Figure 8). (Row 2-4) The difference in potential outcomes between the ground truth and the estimates from LLMs.

Table 2: Chess endgame potential outcome estimates for all actions. We report the *exact model estimate* and *approximate model estimate*. The potential outcome value indicates the expected number of additional moves required to checkmate White. Since Black aims to checkmate the quickest, smaller outcomes are desired.

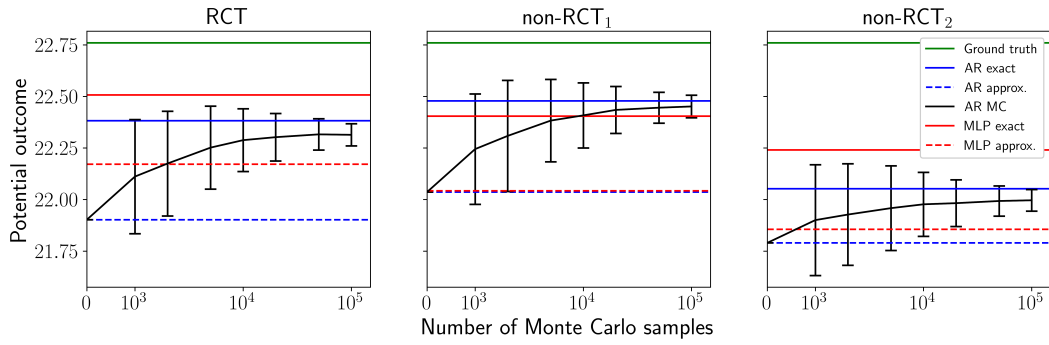
		Potential outcome (Error %)			
		king-king	king-rook	rook-king	rook-rook
Ground truth		22.76	20.18	20.48	17.27
MLP exact	RCT	22.51 (1.1%)	19.96 (1.1%)	19.85 (3.1%)	17.08 (1.1%)
	non-RCT ₁	22.40 (1.6%)	19.85 (1.6%)	20.01 (2.3%)	17.10 (1.0%)
	non-RCT ₂	22.24 (2.3%)	19.90 (1.4%)	19.69 (3.9%)	17.14 (0.8%)
MLP approx.	RCT	22.17 (2.6%)	19.45 (3.6%)	17.72 (13%)	16.18 (6.3%)
	non-RCT ₁	22.04 (3.2%)	19.32 (4.3%)	17.91 (13%)	16.12 (6.6%)
	non-RCT ₂	21.86 (4.0%)	19.31 (4.3%)	17.86 (13%)	16.18 (6.3%)
AR exact	RCT	22.38 (1.7%)	19.75 (2.1%)	19.96 (2.5%)	16.95 (1.9%)
	non-RCT ₁	22.48 (1.2%)	19.87 (1.5%)	20.08 (2.0%)	17.08 (1.1%)
	non-RCT ₂	22.05 (3.1%)	19.88 (1.5%)	19.80 (3.3%)	17.17 (0.6%)
AR approx.	RCT	21.90 (3.8%)	19.19 (4.9%)	17.62 (14%)	15.97 (7.5%)
	non-RCT ₁	22.03 (3.2%)	19.33 (4.2%)	17.95 (12%)	16.15 (6.5%)
	non-RCT ₂	21.79 (4.3%)	19.29 (4.4%)	17.54 (14%)	16.31 (5.6%)

C Chess endgames extra experiments

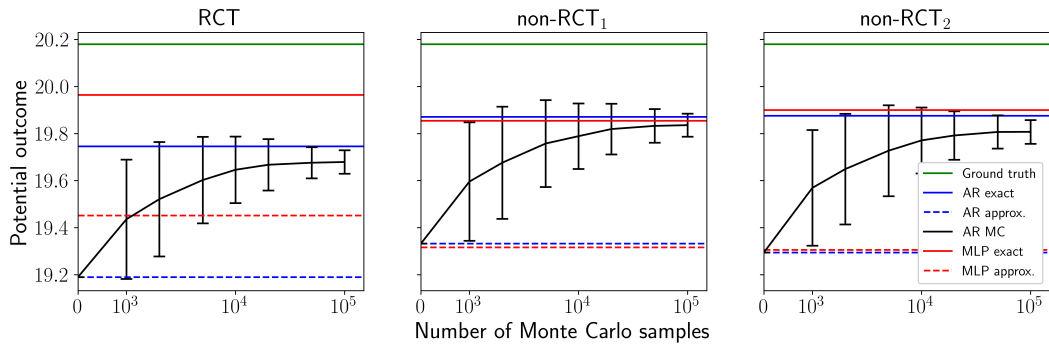
C.1 Potential outcome estimates

We present the potential outcome graphs for the remaining three possible actions: king-king, king-rook, and rook-rook in Figure 10. The model behavior on these actions closely align with the observations for rook-king in Figure 7, indicating that Monte Carlo sampling is effective across various interventions. For all actions, using Monte Carlo sampling achieves better potential outcome estimates when only a subset of the data is available.

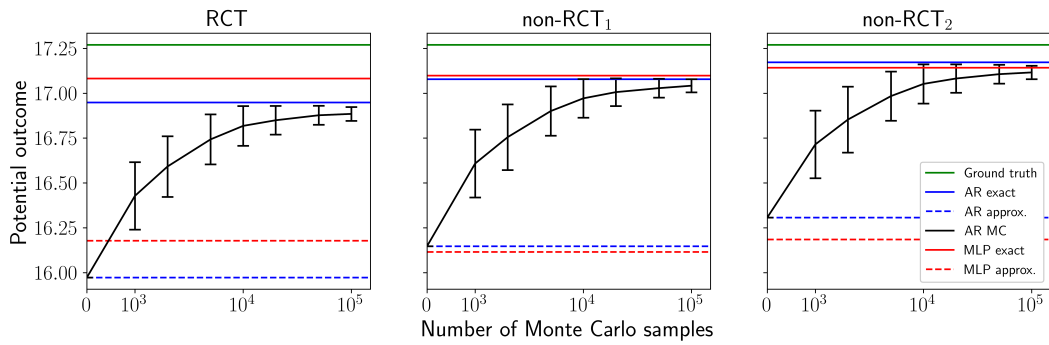
We compare the potential outcome values for all actions in Table 2. We include the *exact model estimates* and *approximate model estimates*. Our autoregressive model performs similarly to the baseline in both these metrics. Hence, our proposed approach adeptly models the outcome, and simultaneously is capable of using Monte Carlo sampling to improve predictions when data is limited. Furthermore, the predictions from all models align with the ground-truth answer to our counterfactual query: on average, moving the rook twice initially leads to checkmate the fastest.



(a) King-king potential outcome estimates.



(b) King-rook potential outcome estimates.



(c) Rook-rook potential outcome estimates.

Figure 10: Potential outcome estimates for king-king (a), king-rook (b), and rook-rook (c) actions.

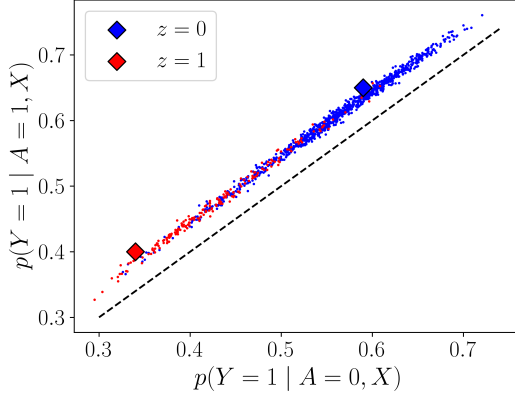


Figure 11: Model conditional outcome distributions given $A = 0$ versus $A = 1$ for the medium confounding case.

Figure 12: Accuracy of title buzziness prediction from abstract using logistic regression.

	Accuracy	Balanced accuracy
BoW	87.95	73.27
BERT	88.57	77.91
GPT2	89.18	81.00

D PeerRead extra experiments

To illustrate the positive predicted ATT on the PeerRead dataset, we compare $p_{\theta}(Y = 1 | A = 1, X)$ against $p_{\theta}(Y = 1 | A = 0, X)$ for all data points using GPT in Figure 11. Our model consistently favours papers containing theorems, regardless of title buzziness.

Additionally, we investigate why our model has strong performance when the outcome is generated from Z and A (cf. Figure 5a), while the input is X and A (cf. Figure 6). We quantify the correlation between the title buzziness and the abstract by training a logistic regression to predict Z from X . For each of our models, we take the final hidden layer output as the vectorized representation of the abstract. We also train a baseline logistic regression model using the bag-of-words (BoW) representation for X . Table 12 demonstrates that X and Z are highly correlated, explaining the high accuracy of potential outcome estimations.